Effect of Supercritical Flow on Scour Characteristics Downstream of Sudden Expanding Stilling Basins

A. M. Negm[*], G. M. Abdel-Aal[*], O. K. Saleh[*] and M. F. Sauida[**]
[*] Associate Professors, Dept. of Water Engrg. & Water Structures, Faculty of Engrg. Zagazig University, Zagazig, Egypt, E-mail: amnegm85@hotmail.com
[**] Post graduated student, Ministry of Water Resources and Irrigation, Telemetry sector, Zagazig, Egypt, E-mail: sauida@hotmail.com

Abstract: The effect of different expansion ratios of sudden expanding stilling basins (SESB) on scour characteristics of downstream (DS) movable soil is investigated in this paper. The flow through sudden expansion is supercritical in the approaching channel with under-gate Froude number ranging from 1.25 to about 5. Three expansions ratios (2.0, 2.5 and 3.0) are considered. The experiments are conducted in a laboratory flume 30 cm wide, 3.5 m Long, and 0.25 m deep. The width of the approach channel is kept unchanged. The collected information are analyzed in terms of the maximum scour depth relative to the gate opening. Both the effects of Froude number and channel expansions are discussed. Different flow and scour patterns are presented and discussed. A prediction equation is developed to compute the depth ratio in terms of the under-gate Froude number, the expansion ratio and the relative gate opening. Good agreement is obtained between the predicted and the measured values using an independent set of experimental data.

Keywords: Hydraulic structures, Stilling basins, Sudden expansion, Scour characteristics, Experimental investigation.

1 Introduction

Many experimenters have been observed that the flow in symmetric expansion is asymmetric. Some of these situations are documented in Graber (1982) who gave an explanation of such phenomenon. He provided a predictive method that agreed well with the experimental observations and then extended it theoretically to analyze proposed corrective measures. The asymmetric flow in sudden expanding stilling basins may cause asymmetric scour downstream the basin where the soil is movable depending upon the flow regime and velocity fields. Nashta et al. (1987) observed that the flow was almost symmetric above movable soil downstream sudden expansion. The flow through sudden expansion in the with Froude numbers ranged from 0.48 to 0.73, uniform sediment size of diameter 0.28 mm and expansion ratios upto 4.5. They concluded that the velocity and scour profiles follow a cosine law for expansion ratio less than 3.0 and a Gaussian distribution for expansion ratio equals 4.5. The

data of Ashida (1963) and Ashida and Miyai (1964) were included in their analysis and follows the same cosine law. They found that the maximum scour depth is a function of the expansion ratio and the Froude number as

$$\frac{D_{sxo}}{y_1} = 0.039F_{r1}\left(\frac{B-b}{b}\right)^{0.44} \quad (1)$$

where D_{sxo} is the maximum of the maximum scour depth that occur at a distance x_o measured from the end of SB in the direction of the flow along the center line, y_1 is the depth of the approaching flow, F_{r1} is the grain Froude number defined by $F_{r1}=V_1/[gd\,(\rho_s-\rho)/\rho]^{0.5}$ where V_1 is the velocity in the approaching channel, g is the gravitational acceleration, d is the medium size of sediment, ρ_s is the density of the sediment material, ρ is the density of the water, B is the width of wider channel and b is the width of the approach channel. They expressed the maximum scour depth along the centerline D_{sx} as follows:

$$\frac{D_{sx}}{D_{sxo}} = \exp\left[-0.238\left(\frac{x}{x_o}-1\right)\right] \quad (2)$$

in which D_{sx} is the maximum scour depth that occur at a distance x measured from the end of SB in the direction of the flow along the center line. Bremen and Hager (1994) conducted two experiments on movable bed in their study on the sudden expanding stilling basin with central baffle sill, one without any appurtenances and the second with central sill for B/b=3.0, F_1=7.0, D_{50}=10 mm. A scour hole is formed under hydraulic jump conditions with a maximum depth of 150 mm at 500 mm downstream from the end of the basin. This scour hole is greatly reduced from 150 mm to 20 mm by using central sill and an end sill with a reduction of 30% for the jump length.

To the best knowledge of the authors, no experimental study has been published to study the effect of sudden expansion under asymmetric supercritical flow conditions on both scour patterns and maximum scour depth downstream of sudden expanding stilling basins. For this reason, this study comes on the line to add some information on these topics.

2 Dimensional Analysis

Figure (1) shows a definition sketch for the phenomena under study. The maximum (max) scour depth, D_s, DS the SB can be expressed as follows:

$$D_S = f(g,\rho,\rho_s,G,V_G,b,B,H_u,D_{50},L) \quad (3)$$

in which D_S is max depth of scour, g is the acceleration due to gravity, ρ_S is the density of the movable soil, G is the gate opening height, V_G is the mean velocity under the gate, H_u is the upstream water depth, D_{50} is the mean particle diameter, and L is the length of apron of the SB.Applying the Buckingham theorem with ρ, G, V_G as repeating variables, Equation (3) can be written in dimensionless form as:

$$\frac{D_s}{G} = f\left(F_G, \frac{H_u}{G}, \frac{B}{G}, \frac{b}{G}, \frac{D_{50}}{G}, \frac{L}{G}, \frac{\rho_s}{\rho}\right) \quad (4)$$

in which $F_G = V_G /(gG)^{0.5}$ is the Froude number under the gate. The effect of the densities ratio, ρ_s/ρ is excluded because only one fluid and one soil is used during the course of experiments. Keeping in mind the properties of the dimensional analysis and divide B/G by b/G to yield B/b which is denoted by e to mean the expansion ratio. Equation (4) is reduced to

$$\frac{D_s}{G} = f\left(F_G, \frac{H_u}{G}, e\right) \quad (5)$$

In Equation (5), H_u/G could be replaced by G/H_u.

3 Experimental Work

The experiments are carried out in a laboratory recirculating flume 0.30 m wide, 0.25 m deep and 3.5 m long. The discharge is measured by means of a calibrated orifice meter installed in the feeding pipeline. The SB model is made from prespex of thickness 10 mm with a length of 1.25 m. The length of the approaching channel is 50 cm while the length of the apron of the SESB is 75 cm. A control sluice gate is made from the same prespex and is used to control the upstream depth and the gate opening. The gate is installed 5 cm upstream the sudden expansion section. The rest of the flume (2.5 m) is covered by sediment consisting of depth equals 7.5 cm sand layer of medium diameter, D_{50} = 1.77 mm. The width of the approaching channel is kept constant to 10 cm, while the width of expanding channel B is variable as 30, 25 and 20 cm to obtain expansion ratios of e=3.0, 2.5 and 2.0 respectively. Different discharges are used (Q = 90.7, 111 and 127.5 L/min) and a range of gate opening such that the Froude number under the gate ranges from 1.25 to about 5.0. A total of about 42 runs are performed. A typical run consisting of leveling the movable soil, allowing a particular fixed tailwater depth in the downstream channel with the control gate in close position. The discharge is adjusted to the desired value and the gate is opened to the desired opening to obtain the required under gate Froude number. During each run the flow pattern is observed and sketched. After about 20 minutes, the water surface profile is recorded. After 30 minutes, the control gate is closed and the pump is switched off. The topography of the movable bed is measured at each 5 cm in the direction of the flow (x direction) and in the widthwise direction or lateral direction (y direction) to enable the study of the scour pattern. Table (1) presents the collected experimental data and shows the experimental conditions of the present work.

4 Results and Discussion

The recorded measurements on the effect of time (T) on maximum depth of scour DS of SESB are plotted in Figure (2). It could be stated that the relationship between D_s/D_{smax} and T/T_{max} is a Log function in the form:

Table 1.Experimental conditions and the collected experimental data

Serial No.	Obser.No.	D_s cm	G(cm)	F_G	Hu(cm)	B(cm)	e	D_{50}(cm)	T(min)	Remarks
1	1	1.6	2.0	2.14	17.0	30	3	0.18	1	
2	2	3.7	2.0	2.14	17.0	30	3	0.18	5	
3	3	4.4	2.0	2.14	17.0	30	3	0.18	30	
4	4	4.8	2.0	2.14	17.0	30	3	0.18	60	
5	5	5.0	2.0	2.14	17.0	30	3	0.18	180	
6	6	5.5	2.0	2.14	17.0	30	3	0.18	360	
7	1	3.7	2.5	1.25	10.0	30	3	0.18	30	Training
8	2	3.8	2.0	1.75	12.5	30	3	0.18	30	Training
9	3	5.2	1.5	2.70	16.5	30	3	0.18	30	Training
10	4	4.4	1.0	4.95	33.0	30	3	0.18	30	Training
11	5	5.0	2.5	1.53	13.0	30	3	0.18	30	*
12	6	3.7	2.0	2.14	17.0	30	3	0.18	30	Test
13	7	4.1	1.8	2.50	21.0	30	3	0.18	30	Training
14	8	4.6	1.5	3.30	27.0	30	3	0.18	30	*
15	9	5.5	2.5	1.77	17.8	30	3	0.18	30	Validation
16	10	6.2	2.0	2.48	23.5	30	3	0.18	30	Training
17	11	7.0	1.8	2.80	27.5	30	3	0.18	30	Training
18	12	7.3	1.5	3.81	25.0	30	3	0.18	30	Training
19	1	2.3	2.5	1.25	9.0	25	2.5	0.18	30	Test
20	2	3.2	2.0	1.75	12.5	25	2.5	0.18	30	Training
21	3	4.8	1.5	2.70	19.5	25	2.5	0.18	30	Training
22	4	5.0	1.0	4.95	33.0	25	2.5	0.18	30	*
23	5	5.3	2.5	1.53	13.0	25	2.5	0.18	30	Training
24	6	4.2	2.0	2.14	19.5	25	2.5	0.18	30	Training
25	7	4.5	1.8	2.50	22.0	25	2.5	0.18	30	Training
26	8	5.0	1.5	3.30	28.0	25	2.5	0.18	30	Validation
27	9	3.0	2.5	1.77	16.5	25	2.5	0.18	30	Test
28	9	0.8	2.0	2.48	23.5	25	2.5	0.18	30	*
29	10	6.2	1.8	2.80	27.5	25	2.5	0.18	30	Training
30	11	7.4	1.5	3.81	34.5	25	2.5	0.18	30	Training
31	1	1.8	2.5	1.25	9.5	20	2	0.18	30	Training
32	2	2.3	2.0	1.75	12.0	20	2	0.18	30	Training
33	3	4.2	1.5	2.70	18.5	20	2	0.18	30	Test
34	4	3.3	1.0	4.95	29.5	20	2	0.18	30	*
35	5	3.0	2.5	1.53	12.5	20	2	0.18	30	Validation
36	6	4.5	2.0	2.14	17.5	20	2	0.18	30	Training
37	7	3.4	1.8	2.50	20.5	20	2	0.18	30	Training
38	8	4.5	1.5	3.30	27.0	20	2	0.18	30	Validation
39	9	5.3	2.5	1.77	26.5	20	2	0.18	30	Validation
40	10	4.7	2.0	2.48	23.5	20	2	0.18	30	Training
41	11	5.3	1.8	2.80	27.0	20	2	0.18	30	Training
42	12	6.4	1.5	3.81	33.0	20	2	0.18	30	Test

* Excluded from the regression model

$$\frac{D_s}{D_{s\,max}} = 0.1147 \log\left(\frac{T}{T_{max}}\right) + 1.059 \qquad (6)$$

This means that the scour depth ratio increases very rapidly with the increase in the time ratio till the maximum scour depth ratio reaches about 85% of the maximum scour then the rate of increase is reduced greatly afterwards. As this study concentrates on the short term scour, the time of each run will be fixed to 30 min as 80% of the scour occurs during this time and the remaining 20% takes very long time till the scour hole reaches the equilibrium state. Figure (3) shows the scour profiles as well as the water surface profiles for the six experiments presented in Figure (2). Initially the bed was leveled and the water surface profile was regular and smooth. Once the scour commenced, the moved soil particles are deposited DS from the formed scour hole causing the shown irregularities of the water surface profile which affect the velocity field that has the major effect on the scour process, Nashta et al.(1987). Figure (3) indicates that the scour at the center line occurs just DS of end of the solid apron of the SB which may endanger the SB and the structure on the long run. However, the maximum scour occurs faraway from the center line of the SESB either on the left or on the right according to the direction of the issuing jet of flow. Figure (4) shows the direction of the issuing jet from under the gate for two cases indicating the fact that the flow through the sudden expanding stilling basin is asymmetric which was documented earlier, for instance, by Graber (1982) and by Bremen and Hager (1994). Figures (5a) to (5c) show the scour patterns due to asymmetric flow for times 5, 60, 360 min respectively. The scour patterns show asymmetric scour. Similar observations could be obtained from Figures (6a) to (6c) at fixed time of 30 min, fixed Froude number of 2.14 and expansion ratios of 2.0, 2.5, 3.0.

Figure (5) shows that the extent of scour and deposition increases as the time increases regarding both depth and distance in the flow direction. The maximum depths of scour are 2.5, 4.0, and 5.0 cm at 5, 60, 360 min respectively. The first 2.5 cm occurs near to the center line on the right hand side (RHS), the 4.0 cm occurs at the RHS of the center line just DS the end of the SESB and the 5 cm scour depth occurs on RHS but away from the end of the SESB at about 25 cm. On the other hand the scour and deposition process for the first 5 min ends at about 55 cm DS the end of the SESB, and ends at 110 cm for the first 60 min while they cover about 250 cm after 360 min. These figures indicated that the time has a major effect on the scour processing which should be carefully considered in the model studies of the existing structures or during design stages when a new structure is to be constructed. Similar observations regarding the max scour could be stated by careful inspection of Figures (6a) to (6c) which present the scour patterns for three different

expansions at fixed F_G =2.14 (Q=111 L/min and G=2 cm) and fixed time of operation at 30 min. As the time is kept unchanged, the extent of scour and deposition process ends at about 93 cm in all cases but the max scour and the max deposition depths are not the same in both magnitude and location. For e=2.0, the max scour occurs on RHS of center line of SESB with max depth of 3.5 cm and another smaller scour hole on left hand side (LHS) with max depth of 2.0 cm and max depth of deposition of 2.0 cm. While for e=2.5, the max scour depth occurs at LHS at a depth of 4.0 cm just DS the end of the apron and another depth 1.5 cm on RHS also just at the end of the SESB where the max depth of deposition in this case is 2.0 cm mostly at the centerline of the channel. The max scour depth for e=3.0 is 3.0 cm and occurs very near to the center line of the channel and just at the end of SESB with max deposition depth of 2.5 cm near to center line on the RHS as the max scour hole. Figure (7) shows the scour profiles along the line of maximum scour at particular F_G and different expansions. Clearly, the smaller expansion produces shallower scour hole. Figure (8) presents the max scour depth ratio D_s/G with the Froude number under the gate for different expansion ratios of 2.0, 2.5, and 3.0. Clearly, the max depth of scour ratio increases linearly with F_G at fixed expansion ratio. On the other hand, at particular F_G the max scour depth mostly occurs at the smaller expansion ratio. Actually, at smaller expansion ratio (e.g. e=2.0 in this case) the tailwater depth for the same F_G is higher which causes more retardation for the incoming jet resulting in weak velocity field and hence the scour depth is reduced. To check these observations, three tests are conducted on the effect of the tailwater depth on the max scour depth assuming the same flow conditions and fixed expansion ratio. These tests indicated that the min scour depths occur at the higher tailwater depths.

Moreover, the relationship between (D_s/G) and (G/H_u) is presented in Figure (9) indicating that the min scour depth occurs at the smaller expansion ratio (e = 2.0 in this case). This figure shows that (D_s/G) decreases with the increase of (G/H_u) at fixed e which means that at fixed G, smaller upstream heads cause little scour because of the issuing jet is more weaker than for larger H_u.

5 Prediction of Max Scour Depth

Using all the collected experimental data on the max scour depth DS of SESB, a prediction model is developed and verified. Seventy percent of the data are used for estimation of the coefficients of the several propsed models relating D_s/G and the different factors of Eq.(5). The remaining 30% of the data are used for validation and test (or verification) of the best models. The regression tool of the Neural Connection (1998) is used to develop the prediction model. Table 2 shows sample results of the conducted regression analysis.From table (2), it is

clear that model number 9 has the greatest value of R^2 =0.857 and the least value of standard error of estimate (SEE) of 0.4476.The final form of this model is

$$\frac{D_s}{G} = 1.13(F_G) - 28.9\left(\frac{D_{50}}{G}\right) + 0.26F_G\left(\frac{B-b}{b}\right) - 3.59\left(\frac{G}{H_u}\right) + 2.1 \quad (7)$$

Table 2. Sample results of the regression analysis

Model no.	Factors	R^2	SEE
1	F_G	0.806	0.4998
2	$\left(\frac{B-b}{b}\right)$	0.034	1.1100
3	G/H_u	0.653	0.6670
4	D_{50}/G	0.582	0.7300
5	$F_G\left(\frac{B-b}{b}\right)$	0.623	0.6960
6	$F_G\left(\frac{B-b}{b}\right)$, F_G, D_{50}/G	0.843	0.4490
7	$F_G\left(\frac{B-b}{b}\right)$, F_G, G/H_u	0.822	0.4780
8	$F_G\left(\frac{B-b}{b}\right)$, D_{50}/G , G/H_u	0.780	0.5300
9	$F_G\left(\frac{B-b}{b}\right)$, F_G, D_{50}/G, G/H_u	0.857	0.4476

Figure (10a) shows the comparison between the measured (D_s/G) and the predicted ones using Eq.(7). Using both estimation and verification data. Clearly good agreement is observed. The residuals of this model is plotted versus both the estimated (70%) and the predicted (30%) in Figure (10b). The residuals show symmetrical distribution around the line of zero scour with mean of -0.011 and standard deviation of 0.438. Also, the residuals are uncorrelated with the predicted values of D_s/G as the correlation coefficient is 0.043 which is negligible. These characteristics of the residuals prove the validity of the model no. 9 which is the best to be used to predict the maximum scour depth DS of SESB. The proposed model, Eq (7) is used to predict the max scour depth for different F_G of 1.5, 2. 2.5, 3, 3.5, 4 and 4.5 where e=2.0, 2.5 and 3.0. These results are presented in Figure (11). Finally Figure (12) shows the maximum

scour depth according to Eq (1) developed by Nashta et al. (1987). The discrepancy between these results are mainly due to the effect of regime, the sediment size, the extent of the solid apron where no solid apron is used for Nashta et al. study and the other operation conditions.

2- The scour pattern is not symmetrical and the max scour occurs either on the left or on the right from the longitudinal center line of the channel DS of SESB.

3- The deposition and max deposition depth are also not symmetrical.

4- The lower expansion ratio yields smaller values of the max scour and vice versa.

5- Prediction model is developed and verified for computing the maximum scour depth knowing the F_G, B/b, G/H_u, and D_{50}/G.

6- The developed model shows good agreement between measured and predicted values.

7- Long term scour should be considered for physical models of such structures as the time shows major effect on the max scour and on the extent of the scour and deposition process.

8- It is recommended to conduct an extensive experimental study to investigate the effect of expansion ratio on the other characteristics of scour and deposition process.

9- It is recommended to investigate the effect of central baffle sill at different locations with different heights using different expansions on the scour processing DS of SESB.

6 Conclusions

The present study highlighted the following conclusions:

1- The scour pattern DS of sudden expanding SB is a function of F_G, B/b, G/H_u and D_{50}/G at fixed sediment size and fixed operation time.

10- Also, it is recommended to test the effect of end sill on scour DS of SESB.

References

Ashida, K. (1963), Study on the stable channel through constrictions, Annual Report of Disaster Prevention, Research Instituto, Kyoto University, Kyoto, Japan.

Ashida, K. and Miyai, H. (1964) Study on the sedimentation in an abrupt expansion, Annual Report of Disaster Prevention, Research Instituto, Kyoto University, Kyoto, Japan.

Bremen, R. and Hager, W.H. (1994), Expanding stilling basin Proc. Instn Civ.Engrs Wat.,Marit.&Energy, 1994, 106 , Sept., 215-228.

Graber, S.D. (1982), Asymmetric flow in symmetric expansion; Journal of Hydraulics Div., Proc. ASCE, Vol. 108, No. HY10, Oct. pp.1082-1101.

Nashta, C.F., Swamee, P.K. and Garde, R.J. (1987), Subcritical flow in open channel expansions with movable bed, Journal of Hyd. Research.Vol 25,.No.1, 89-102.

Neural Connections (1998), SPSS Inc./Recognition Systems Inc., ANNs software and user manuals.

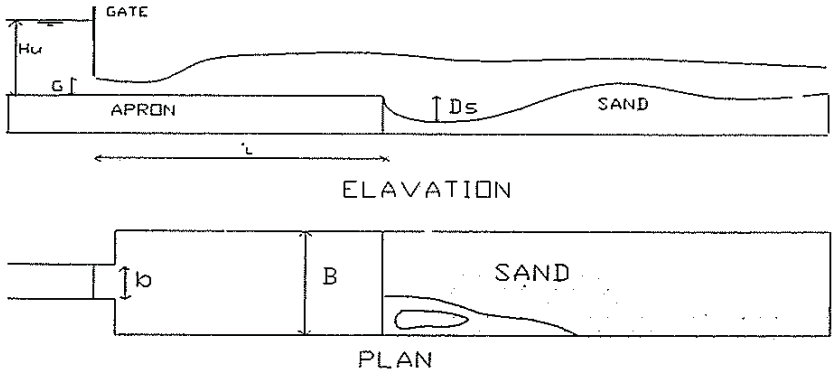

Figure 1. Definition sketch showing scour DS sudden expanding SB.

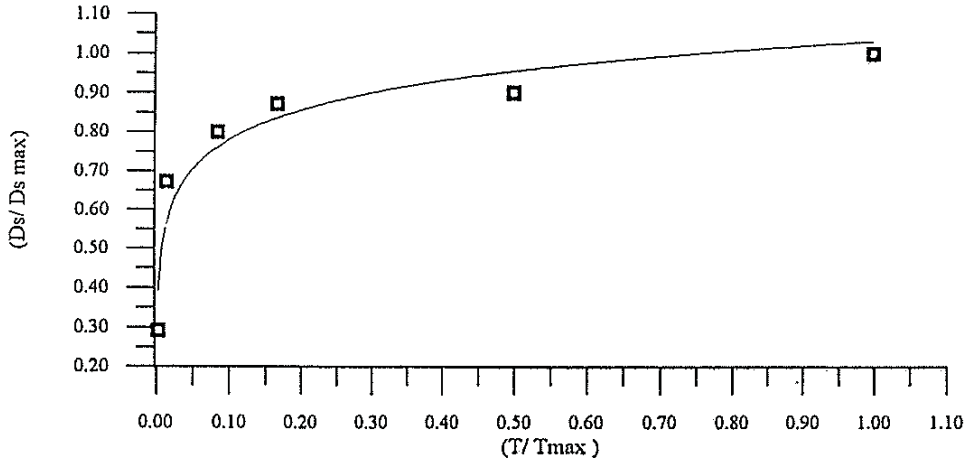

Figure 2. Effect of time of operation on maximum scour depth DS of SESB

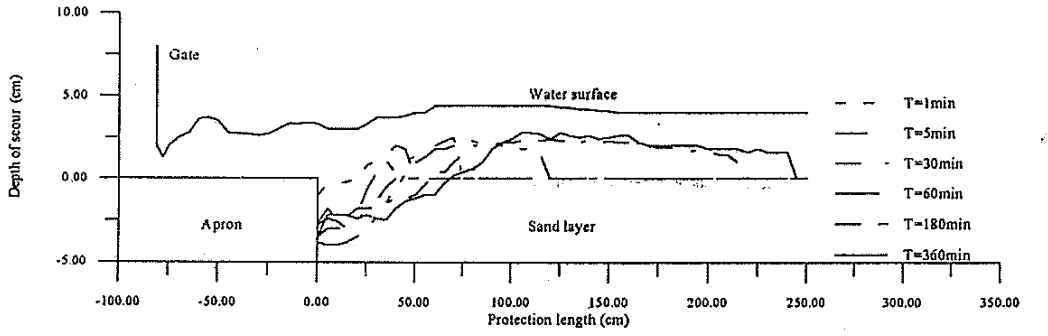

Figure 3. Water surface profile at e=3.0 and F_G=2.14, (Q=111 L/min and G=2 cm)

(a) e=2.0 (b) e=3.0

Figure 4. Two typical flow patterns occurs at the same F_G=2.14 (Q=111 L/min and G=2 cm)

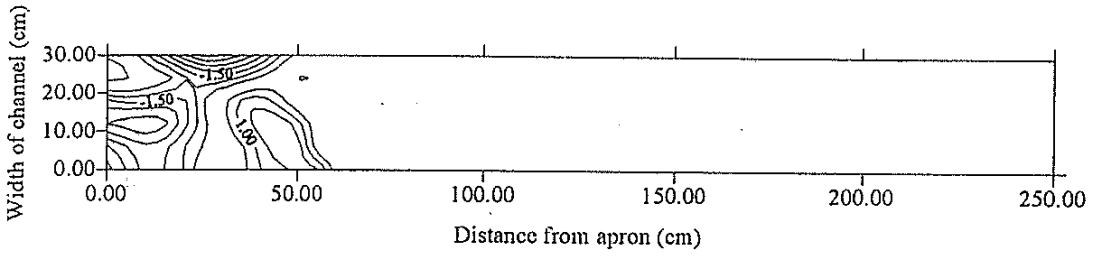

(a) time = 5 minutes

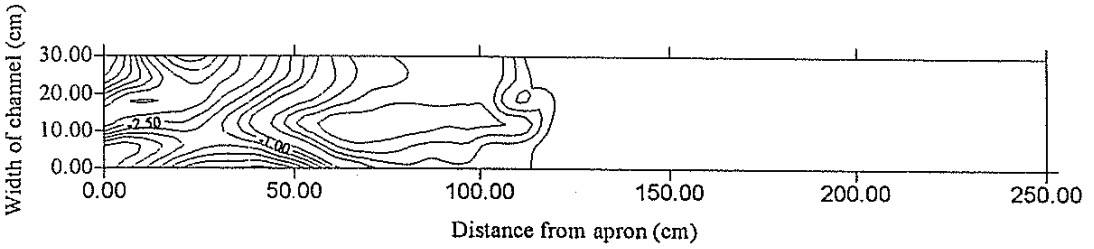

(b) time = 60 minutes

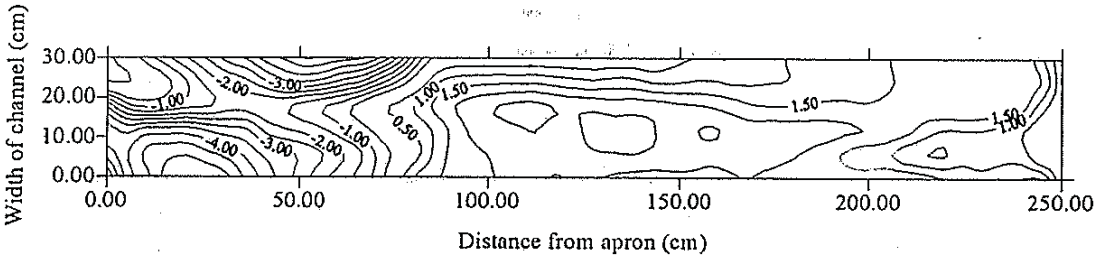

(c) time =360 minuts

Figure 5. Scour patterns for different times of operation at e=3.0 and F_G=2.14 (Q=111 L/min, G=2 cm)

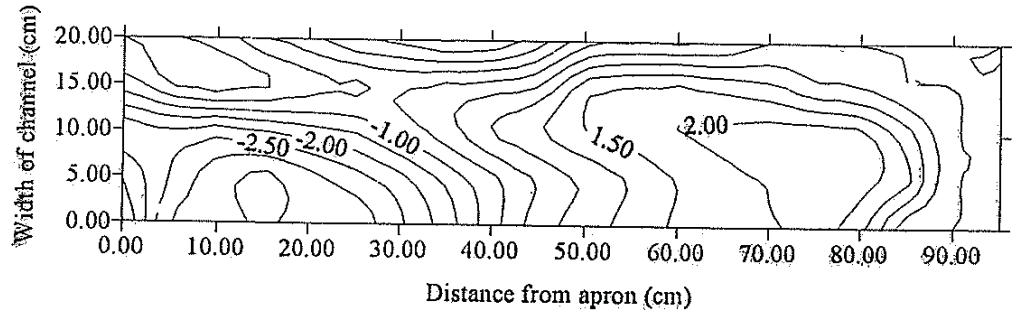

(a) e=2.0

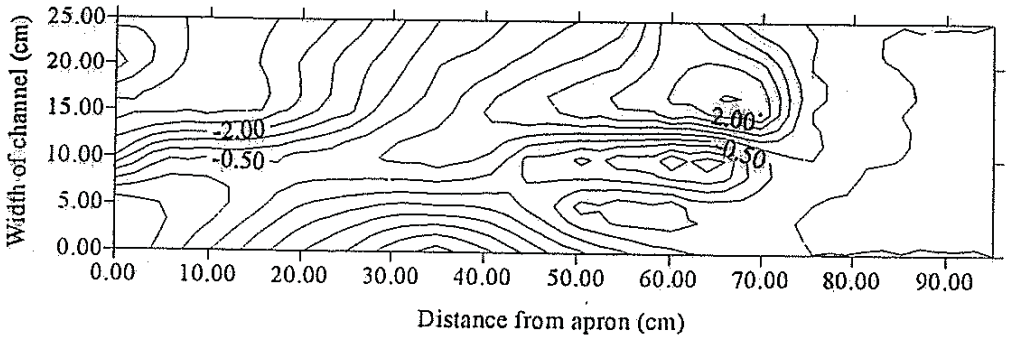

(b) e = 2.5

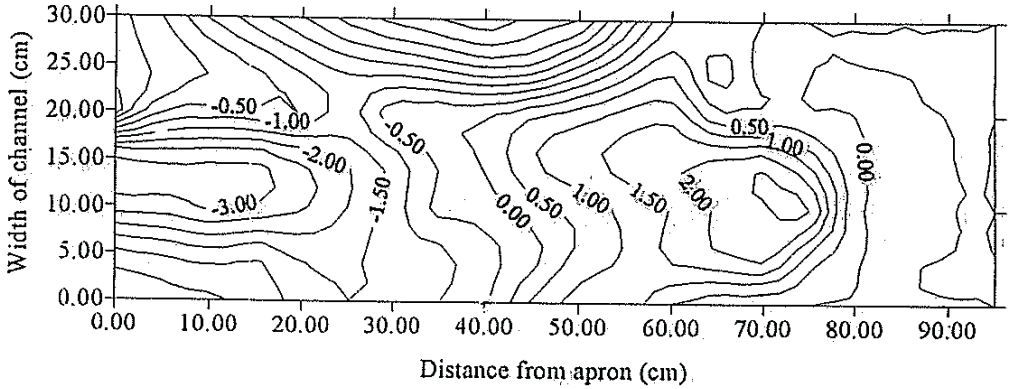

(c) e=3.0

Figure 6. Scour patterns Ds of SESB for different expansions at fixed time of operation (30 min) and at F_G=2.14 (Q=111 L/min and G=2 cm)

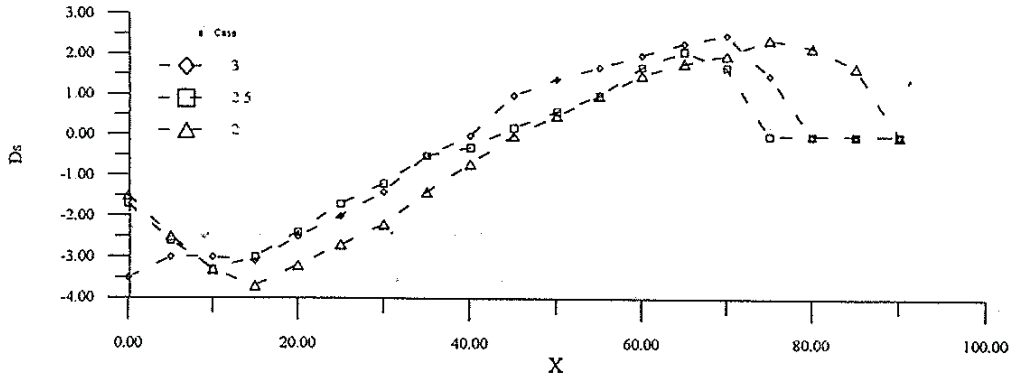

Figure 7. Scour profiles at the line of maximum scour for different expansion ratios at particular F_G=2.14 (Q=111 L/min and G=2 cm)

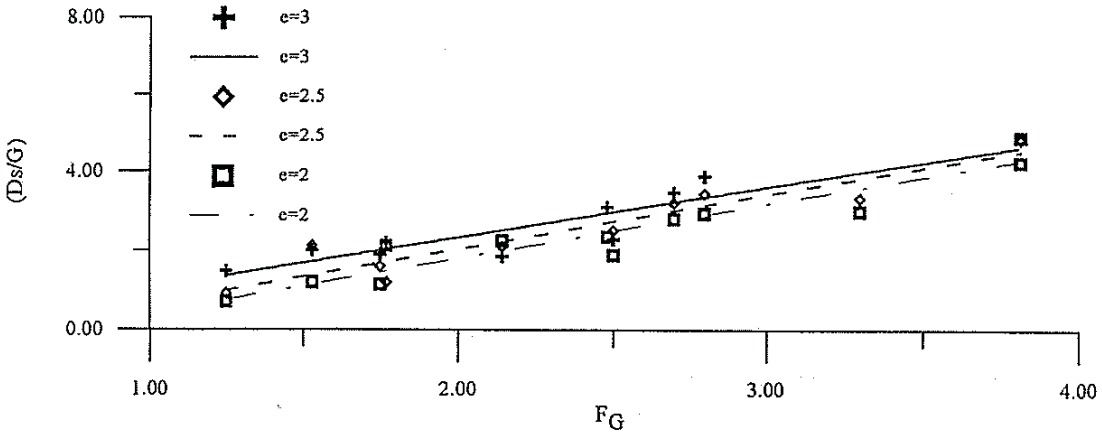

Figure 8. Relationship between D_s/G and F_G for different expansions

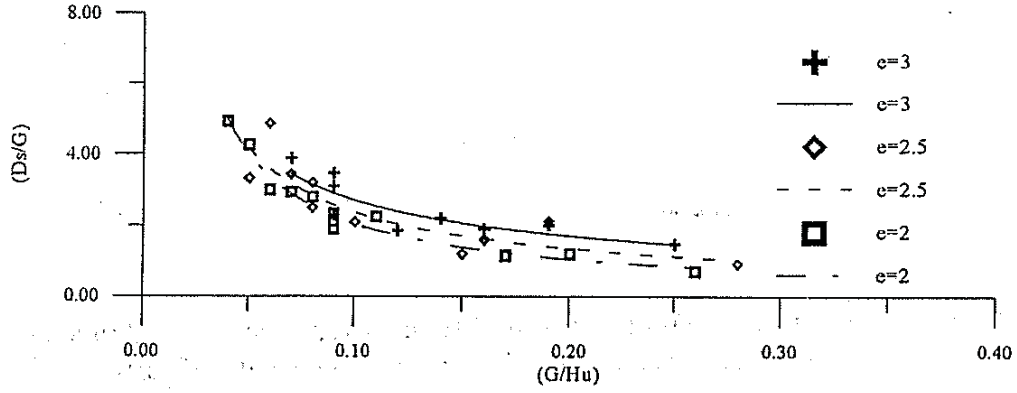

Figure 9. Relationship between D_s/G and G/H_u for different expansions

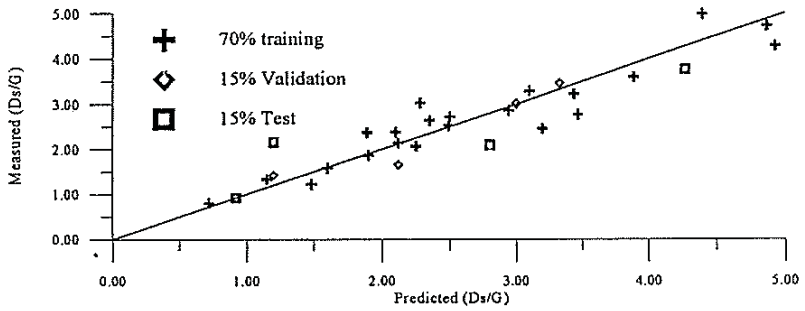

Figure 10a. Comparison between measurements and prediction of Eq.(7)

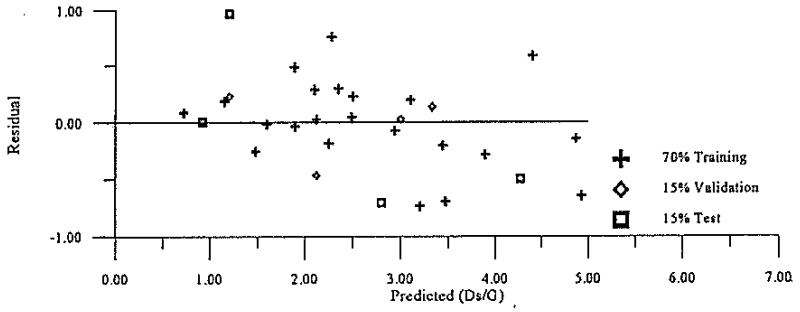

Figure 10b. Residuals versus predicted maximum depth

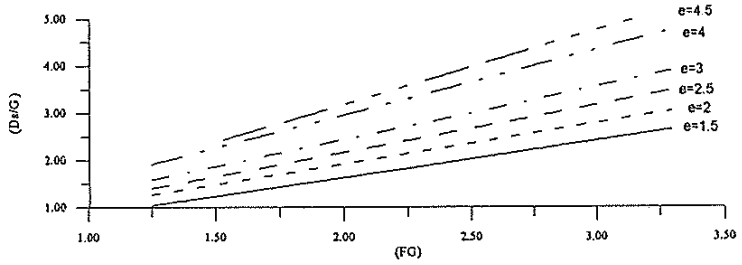

Figure 11. Predicted D_s/G using Eq.(7) versus F_G for different expansions

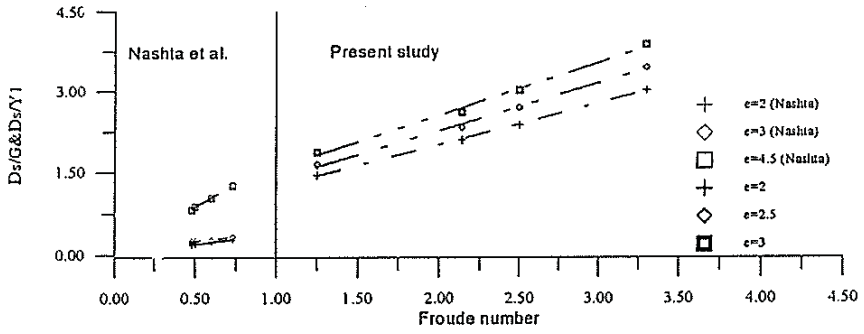

Figure 12. Comparison between maximum scour depth
For present study and that of Nashta et al. (1987)